Iron oxides in laterites : a combined mineralogical, magnetic, and diffuse reflectance study

PDF erstellt am: **17.05.2024**

Persistenter Link: https://doi.org/10.5169/seals-58465

Iron oxides in laterites: a combined mineralogical, magnetic, and diffuse reflectance study

by *N. Malengreau[1], P.G. Weidler[2] and A.U. Gehring[2]*

Abstract

The combination of X-ray diffractometry (XRD), diffuse reflectance spectroscopy (DRS) and isothermal remanent magnetization (IRM) was used to identify the mineralogy of laterites from southern Mali, consisting of a saprolite and a ferriferous duricrust. Quartz, gibbsite, kaolinite, and vanadian muscovite were detected by XRD. Comparison of DRS and IRM data indicated magnetite as the only ferrimagnetic phase. All goethites from the saprolite contained an Al-amount of approximately 14.7 mole% Al. In the duricrust, two types of goethites occurred, a pure one and one with an Al-substitution of 12.1 mole% as indicated by XRD and DRS. X-ray diffractometry revealed an Al-substitution in hematite of approximately 6.7 mole%, but no correlation between Al-substitution and band position in DRS was found. More calibration is necessary to improve the analysis of Al-substitution in natural hematite by DRS.

Keywords: laterite, Fe-oxide, Al-substitution, X-ray diffraction, Rietveld analysis, magnetization, reflectance spectroscopy.

Introduction

In laterites which are highly weathered tropical soils, the iron oxides goethite (α-FeOOH) and hematite (α-Fe$_2$O$_3$) are major components, whereas magnetite (Fe$_3$O$_4$) and maghemite (γ-Fe$_2$O$_3$) are minor constituents. Generally, these major components can easily be identified and characterized by X-ray diffraction (e.g. SCHWERTMANN, 1988). Problems in the identification of iron oxides in natural samples can arise if their concentrations are relatively low, or the mineral composition of the sample leads to an overlap of diagnostic diffraction lines. This problem can be severe for natural ferric oxides in which Fe(III) substitution by cations such as Al(III) causes shifts in peak positions (e.g. NORRISH and TAYLOR, 1961). In addition, small crystal sizes of goethite and hematite lead to a broadening of the diffraction lines. This can be the case for goethite in laterites where it occurs together with gibbsite, quartz, kaolinite and mica. In XRD, numerical methods have been used to fit measured peak profiles (NAIDU and HOUSKA, 1982). Such computation permits the separation of overlapping diffraction

lines. This procedure often leads to no unique solution to fit measured peaks, and, therefore, to ambiguity in mineralogical interpretation. A better description of mineral phases (e.g. cell-parameters) can be obtained by using the Rietveld method (YOUNG, 1993). This method has been successfully applied if the mineral phases are in concentrations of more than 1 weight%, their chemical compositions are known, and no significant structural disorder exists (BISH and JONES, 1991). To improve the identification of iron oxides in natural samples, different chemical and physical separation techniques have been applied (SCHWERTMANN, 1964; HUGHES, 1982). An alternative non-invasive approach is the use of the Rietveld method in combination with spectroscopic and/or magnetic methods, which can provide specific information on iron oxides (e.g. COEY, 1988; GEHRING and KARTHEIN, 1990).

Recently, MALENGREAU et al. (1994) have shown that diffuse reflectance spectroscopy (DRS) in the UV-visible range is a powerful tool to detect and identify ferric iron concentrations down to 100 mg kg^{-1}. Iron (III) in minerals is generally detectable in the UV range (200–400 nm).

[1] ESPM-ESD, University of California, 108 Hilgard Hall, Berkeley, CA 94720, USA.

[2] Institute of Terrestrial Ecology, ETH Zürich, Grabenstrasse 3, CH-8952 Schlieren, Switzerland.

In the case of iron oxides, the visible range (400–800 nm) can provide additional information about their nature. Almost all these oxides display a weak absorption near 660 nm (SHERMAN and WAITE, 1985) and one or two bands at lower wavelengths (470–550 nm) in the visible range. The latter are used to identify and characterize major types of iron oxides except magnetite (HUNT et al., 1971; MALENGREAU et al., 1994). Magnetite is opaque and uniformly absorbs radiation in the UV-visible range (HUNT et al., 1971). This mineral phase can, however, be detected easily by magnetic methods (e.g. COEY, 1988). The combination of DRS and magnetic methods thus permits the identification of the whole range of naturally occurring iron oxides.

The purpose of this paper is to describe the application of DRS combined with XRD and magnetic methods as additional tools for identification and characterization of iron oxides in multimineral systems. A laterite was used as an example. .

Samples and methods

The samples were collected from a laterite exposed in exploration pits at Tabakoroni in the savannah woodland of southern Mali. Since early Tertiary, lateritization of Precambrian bedrock produced a weathering mantle, which consists of a thick kaolinite-rich saprolite capped by a reddish nodular duricrust (Munsell hue: 2.5YR 4/6). Erosional dissection of the weathering mantle led to the exposure of the saprolite and subsequent leaching of iron oxides along a footslope (GEHRING et al., 1994). This process is well indicated by a mottled zone along the slope and the formation of a pallid zone mainly consisting of a homogeneous greyish-white saprolite (10YR 7/1) at the downslope. For the mineralogical investigations, samples (LS3, LS5, LS9, and LS10) from the mottled and the pallid zones were collected. In addition, samples (OS1 and DC1) from an ochreous saprolite (10YR 6/8) and the above duricrust of the intact weathering mantle were taken.

The duricrust and the five saprolite samples were characterized by powder X-ray diffractometry (XRD, SCINTAG XDS 2000) using CuKα radiation and a Peltier-cooled lithium drifted silicon detector. The samples were ground to 10 µm, suspended in acetone and then put on glass slides with a pipette. Diffractograms were recorded between 2 and 52° 2Θ with steps of 0.025° and 15 s counting time per step. The quartz in the samples was taken as an internal d-spacing standard to correct peak positions. The structure refinement was performed by using the program WYRIET

(version 3) based on the Rietveld method (cf. SCHNEIDER, 1987). This method was applied to calculate unit cell parameters in order to analyze the Al-substitution in the iron oxides. The Al-substitution of goethite was determined using the formula for the c-parameter proposed by SCHWERTMANN and CARLSON (1994) and for hematite the equation for the a-parameter by STANJEK and SCHWERTMANN (1992). The standard deviations (ESD) of the calculated Al-substitutions were estimated from the reported ESDs of these equations and the ESDs of unit cell parameters determined by the Rietveld program. The magnetic properties of the iron oxides were determined by isothermal remanent magnetization (IRM). The IRM was produced in progressively increasing magnetic fields with a magnetic induction up to 1 Tesla, and was measured on a Molspin magnetometer (e.g. COEY, 1988).

Diffuse reflectance spectra of six samples were obtained between 200 and 800 nm in a digital form and at room temperature with a CARY 2300 spectrophotometer fitted with a 10-cm-diameter integrating sphere coated with halon. Diffuse reflectance measurements were made relative to halon. The spectral resolution varied from 1 nm in the UV region to 2 nm in the near IR region. The wavelength accuracy of the spectrometer, checked by using emission line peaks from deuterium, was within ± 0.1 nm in the UV and visible regions. The Kubelka-Munk formalism (remission function) was used to model the light scattered. Noise reduction of the experimental spectra was performed by fitting a cubic spline function to each spectrum (DUNFIELD and READ, 1972). Details of the spline smoothing procedure were described elsewhere (e.g. REINSCH, 1967). Second derivative functions were then calculated using a numerical method (HUGUENIN and JONES, 1986). The second derivative permitted ill-defined absorption bands to be accurately located and overlapping bands in experimental spectra to be resolved (CAHILL, 1979). The positions of absorption bands were indicated by minima on the second derivative curves. These positions were determined with an accuracy of ± 2 nm, considering the spectrometer resolution and errors caused by mathematical procedures such as smoothing and derivation.

Results

The mineralogical analysis by XRD showed kaolinite and quartz as major phase in all samples (Fig. 1). Gibbsite occurred as component in DC1, LS3, and LS9. In all saprolite samples a 2M1 muscovite
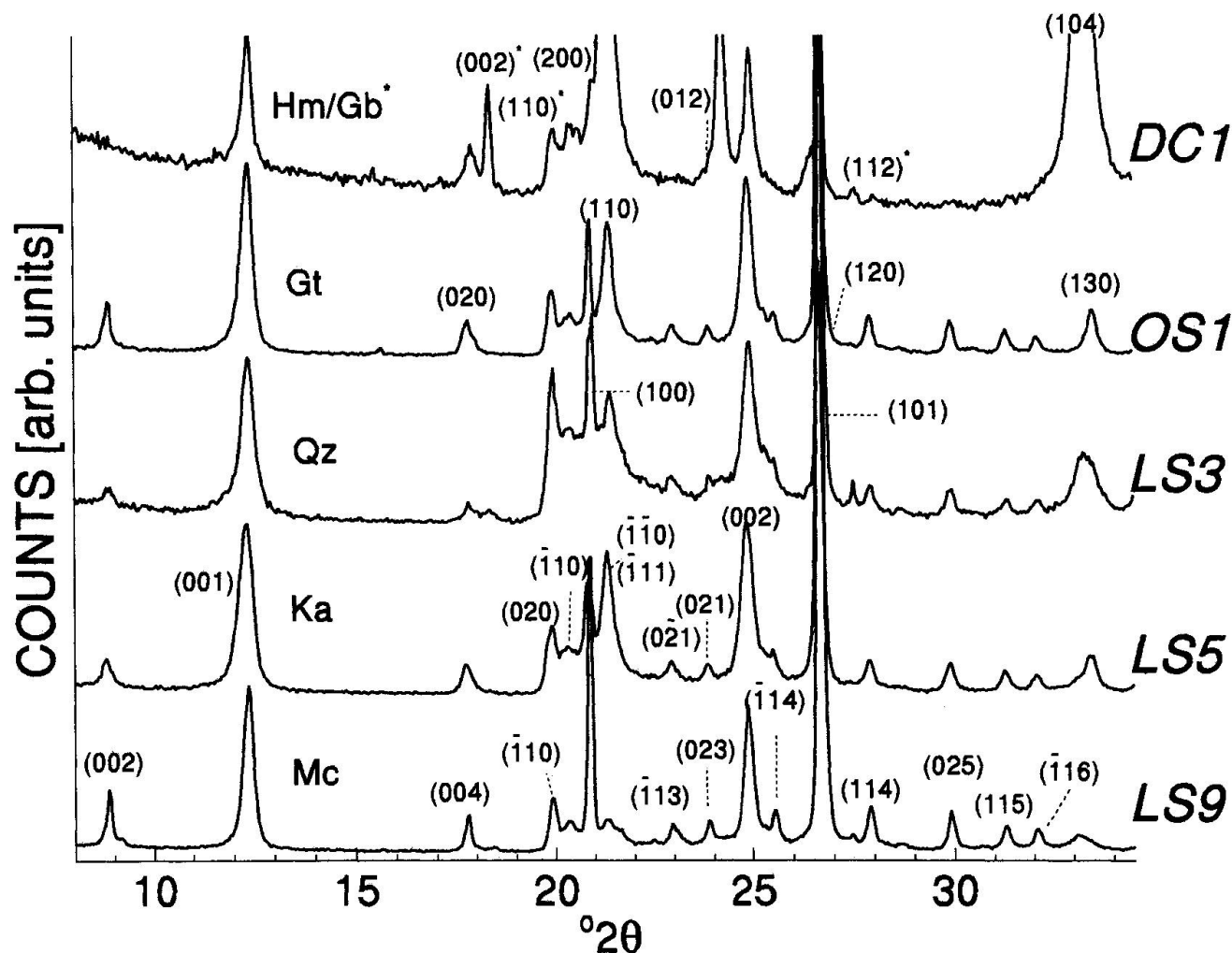
Fig. 1 X-ray diffraction of laterite samples. The diagnostic diffraction lines are indicated for muscovite (Mc) in LS9; kaolinite (Ka) in LS5; quartz (Qz) in LS3; goethite (Gt) in OS1; hematite (Hm) and gibbsite (Gb, marked with asterisks) in DC1.

was found. Table 1 shows unit cell parameters of these mineral phases obtained by structure refinement. The parameters differed in the mean by 0.15% from data published by the International Centre for Diffraction Data (ICDD; BERRY et al., 1986). The refined a-parameter of the muscovite

Tab. 1 Mean values of the mineralogical properties of the non-ferriferous components in the duricrust and the saprolite samples; standard deviations in parantheses. The differences between refined and literature values are expressed in %.

Minerals	Unit cell parameters [nm]			Angles [°]		
	a	b	c	α	β	γ
Quartz [1]	0.4911 (2) -0.04%	– –	0.5405 (3) -0.01%	90 –	90 –	90 –
Kaolinite [2]	0.518 (1) -0.47%	0.892 (1) 0.44%	0.739 (1) -0.21%	91.7 (2) -0.01%	104.4 (1) -0.46%	90.0 (1) -0.05%
Muscovite [3]	0.5194 (3) -0.15%	0.8988 (6) -0.53%	2.0061 (5) -0.03%	90 –	95.77 (4) -0.02%	90 –
Gibbsite [4]	0.870 (3) 0.47%	0.5070 (4) -0.03%	0.971 (2) -0.03%	90 –	94.59 (4) -0.02%	90 –

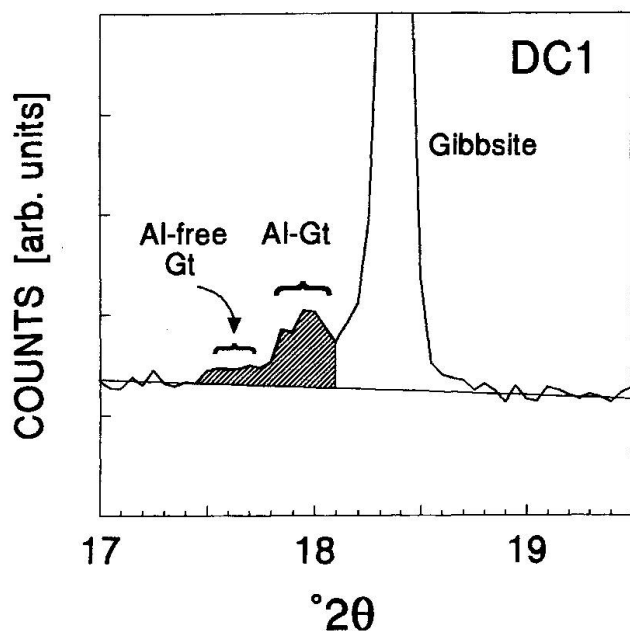Reference ICDD: [1] 33-1161; [2] 14-164; [3] 19-814; [4] 33-18.

Fig. 2 Narrow range scan obtained from a DC1 sample with (020) peaks (shaded) of two goethite types.

in the saprolite was 0.5194 nm and significantly larger than the 0.5119 nm reported for a standard 2M1 muscovite (BERRY et al., 1986; ICDD 6-263). Hematite as major component was found in the duricrust. For this hematite, an Al-substitution of less than 1 mole% was calculated. In LS3, LS5, and LS9 hematite occurred as minor constituent with Al-amount of 13.2 ± 3.4, 6.0, and 6.0 ± 2.7 mole%, respectively. The cell-parameters of hematite in sample LS5 could not be well refined due the low concentration and therefore, only a mean value was calculated. In the other samples no hematite was detected by XRD. The characteristic diffraction lines of goethite interfered with the (004) of mica, (111) of kaolinite, (101) of quartz, and (130) of hematite (Fig. 1). Goethite was found in DC1, OS1, LS3 and LS5. The Rietveld refinement of goethite led to unit cell parameters with standard deviations of less than 0.5%. The calculated Al-substitution was 12.6 ± 0.6 mole% for OS1, 18.2 ± 0.9 mole% for LS3, and
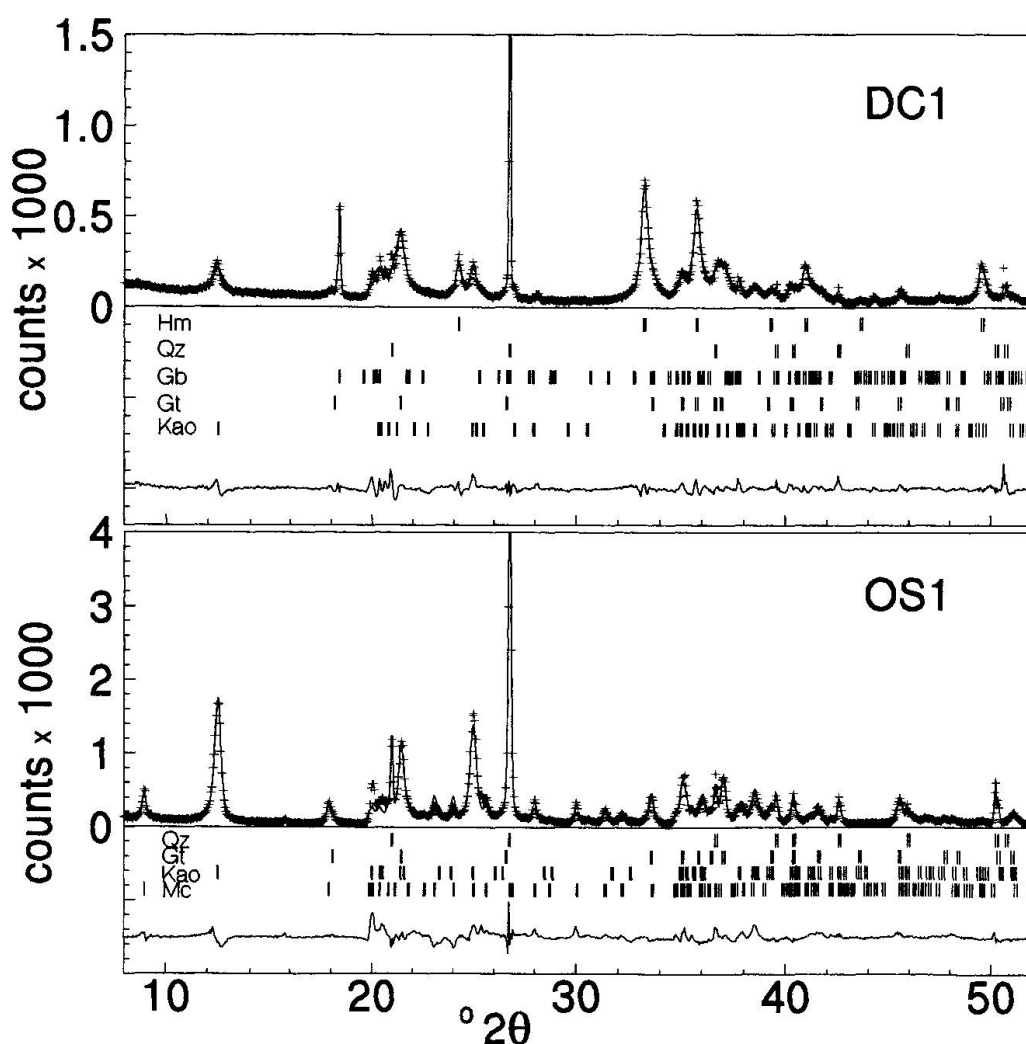

Fig. 3 Rietveld refinement in sample DC1 and OS1 with the measured profiles (+) and calculated profiles (solid line), and their difference curves. Peak positions of each mineral phase are indicated by vertical bars.
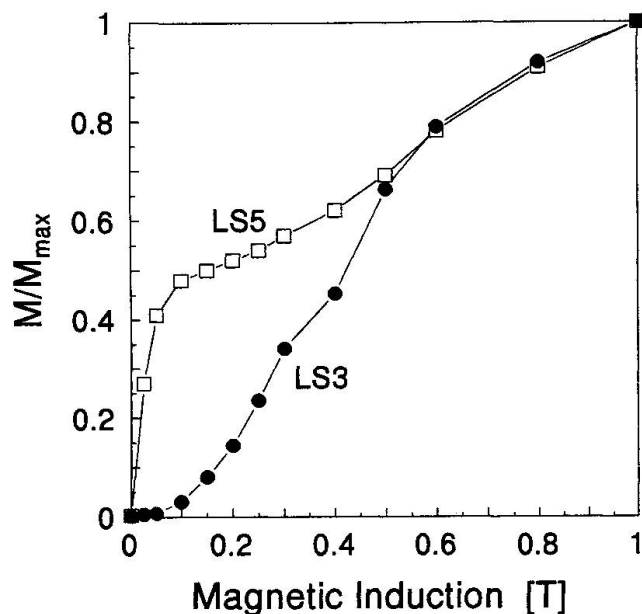
Fig. 4 Isothermal remanent magnetization acquisition of sample LS3 (closed circles) and sample LS5 (open squares).

13.4 ± 0.7 mole% for LS5. In the duricrust, goethite was a minor component. Detailed X-ray analysis of the angle range between 17 and 19.5° where the goethite (020) peak was not overlapped, revealed two peaks (Fig. 2). These peaks could be attributed to two goethites with different Al substitutions. The intensity of (020) peak assigned to the Al-free goethite according to its b-parameter, indicated insufficient amounts to permit successful incorporation of this mineral phase in the Rietveld refinement. By contrast Rietveld refinement of an aluminous goethite was successful and yielded a substitution of 12.1 ± 1.5 mole%. No significant amount of amorphous or poorly crystalline ferric phases were found in the laterite samples as indicated by the difference curves obtained by the Rietveld refinement (Fig. 3).

For LS10, the concentration of magnetic minerals was below the detection limit of the IRM experiments. The IRM acquisition curve of the other samples consisted of low and/or high coercivity components. The high coercivity components were far from saturation in the maximum field applied as shown for samples LS3 and LS5
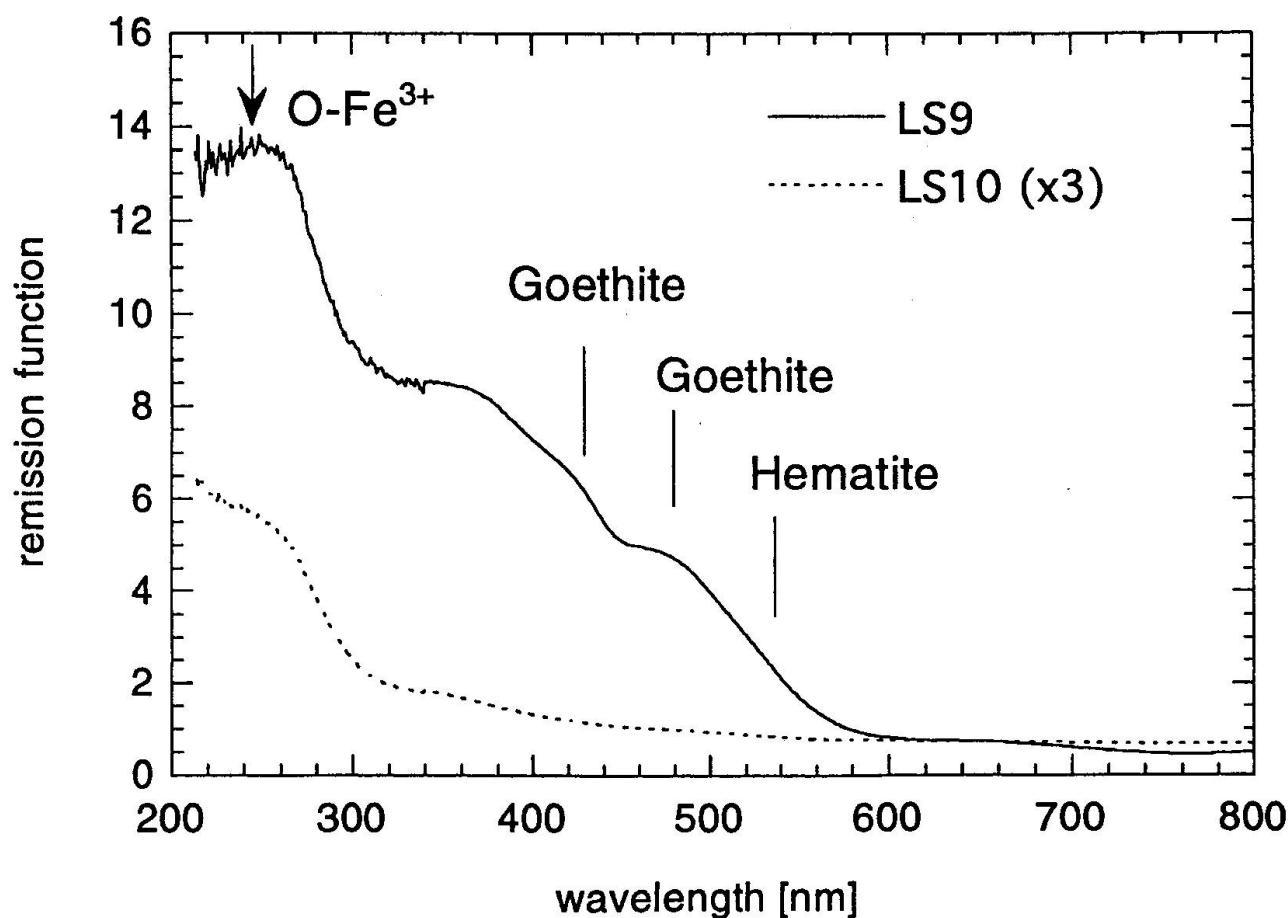

Fig. 5 Diffuse reflectance spectra of LS5 and LS10 samples in the UV-visible range. Arrows indicate the positions of absorption bands assigned to Fe^{3+}–O charge transfer and to the various Fe-oxides. Spectrum of sample LS10 is increased by a factor of three.
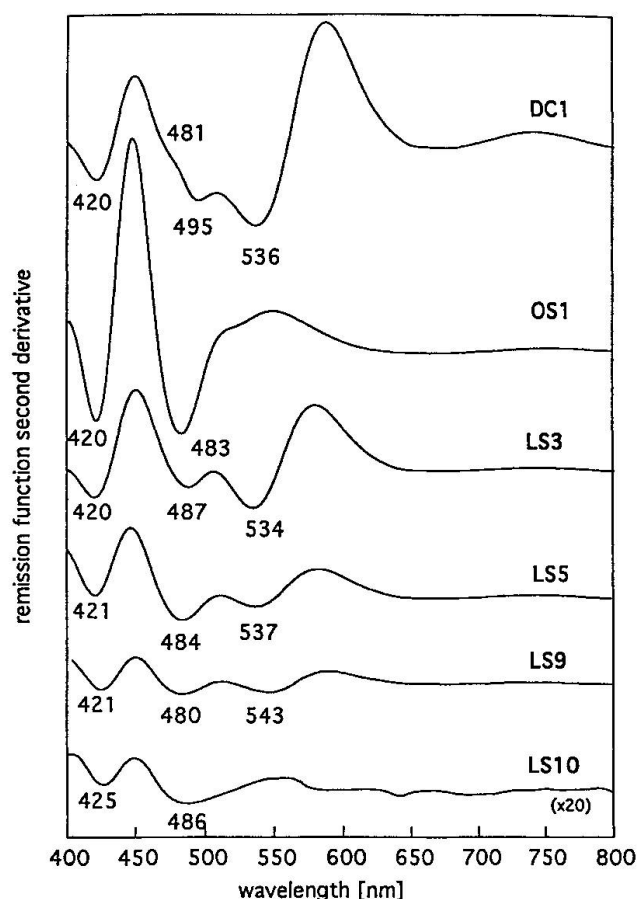
Fig. 6 Second derivative curves in the visible range of the duricrust sample (DC), the ochreous saprolite (OS) and the exposed saprolite (LS). Curve of sample LS10 is increased by a factor of 20.

(Fig. 4). The presence of a low coercivity component was indicated by a steep increase of magnetization in fields below 0.2 T. The relative contribution of the low coercivity phases to the IRM acquisition curves varied. The highest value was found for LS5, whereas no significant contribution was detected for LS3 (Fig. 4).

The spectra of all samples in the visible and UV ranges exhibited absorptions due to iron in its trivalent form (Fig. 5). In the UV range, absorption at about 275 nm could be assigned to Fe^{3+}–O charge transfer (KARICKHOFF and BAILEY, 1973). The absorption edge at about 350 nm, which was best developed in LS5, could be attributed to Ti–O charge transfer in anatase (MALENGREAU et al., 1995). In the visible range below 600 nm, bands were observed that were diagnostic for ferric oxides. These absorption bands were very weak in LS10 (Fig. 5). Second derivative spectra for all samples showed two major bands at approximately 420 nm and between 480 and 495 nm (Fig. 6). The highest intensity of these bands was observed in OS1 and the lowest intensity occurred in

LS10. These absorption bands were characteristic of goethite; the absorption at approximately 420 nm corresponded to the $(^6A_1) \rightarrow (^4E,^4A_1(^4G))$ transition and the one at higher wavelengths could be attributed to the $2(^6A_1) \rightarrow 2(^4T_1(^4G))$ transition. In all saprolite samples, the latter transition band was found at wavelengths between 487 and 480 nm (Fig. 6). In DC1, this transition band occurred at 495 nm and in addition a shoulder at approximately 481 nm was found. Samples from the saprolite along the slope and the duricrust exhibited also a band with a position varying between 534 and 543 nm. Absorptions in this range were typical of hematite and were attributed to the $2(^6A_1) \rightarrow 2(^4T_1(^4G))$ transition (SHERMAN and WAITE, 1985).

Discussion

The non-ferriferous major components in the laterite profile such as quartz, gibbsite, kaolinite, and muscovite can be only detected by XRD. The latter mineral is most likely a vanadian muscovite, since the refined value of the a-parameter is similar to 0.5202 nm, the value found for such mica (SNETSINGER, 1966). The characterization of muscovite agrees well with electron spin resonance spectroscopic data, which showed that this mineral phase contains four-valent vanadium (GEHRING et al., 1993).

Diffuse reflectance spectroscopy exhibits that all samples contain goethite and/or hematite. These two minerals are also indicated by the high coercivity behavior in the IRM curves. In all samples goethite is found by DRS whereas in the samples LS9 and LS10 the concentration of this mineral phase is below the XRD detection limit. The shift of the $2(^6A_1) \rightarrow 2(^4T_1(^4G))$ transition towards lower wavelengths for goethite from the saprolite can be explained by Al-substitution (KOSMAS et al., 1986). Comparing the position of a line for a pure goethite at approximately 493 nm (MALENGREAU et al., 1994) with those obtained from the laterite samples suggests that all goethites are Al-substituted. Since the DRS measurements have an accuracy of $\pm$ 2 nm, the Al-substitution in goethites of the saprolite samples are not significantly different. The Al-substitution in goethites obtained from XRD data for samples OS1, LS3, and LS5 also show no significant difference. Comparing the XRD results with the DRS data, a shift of approximately 10 nm corresponds to 14.7 mole% Al. For synthetic goethites, KOSMAS et al. (1986) found a negative correlation between the second derivative band position and the Al-substitution. In their study, a shift of 10 nm cor-

responded to an Al-substitution of 12 mole% and is in good agreement with the values obtained for goethites in the saprolite. The DRS spectrum of DC1 with a band at 495 nm and a shoulder at approximately 481 nm argues in favor of two different goethites with respect to their Al-substitution. According to KOSMAS et al. (1986) the band at 495 nm corresponds to a pure goethite whereas the shoulder can be attributed to a goethite with Al-substitution of approximately 18 mole%. This finding is in good agreement with the XRD data which also exhibit two types of goethite differing in their Al-amounts. In laterites, the occurrence of two types of goethites provides evidence for different chemical environments during the genesis of the duricrust (e.g. TARDY and NAHON, 1985).

Hematites in the duricrust and in the saprolite samples contain approximately 6.0 mole% Al indicated by XRD. KOSMAS et al. (1986) showed that Al-substitution leads to a shift of the $2(^6A_1) \rightarrow 2(^4T_1(^4G))$ transition towards lower wavelengths. For the quantification, these authors used the position of the maximum of the second derivative spectrum at approximately 600 nm. They reported a shift of 10.4 nm for an Al-substitution of 12.5 mole%. According to this correlation, the maximum positions below 585 nm for the samples from the laterite profile correspond to Al-substitutions of more than 25 mole%. Such a high substitution is known neither for synthetic nor for natural hematites (e.g. BARRON et al., 1984). MALENGREAU et al. (1994) used the minimum band position of the $2(^6A_1) \rightarrow 2(^4T_1(^4G))$ transition for identification of hematite. For pure hematite, they found a position at 542 nm which is close to the 550 nm position reported by SHERMAN and WAITE (1985). The minimum band positions for DC1, LS3, and LS5 are shifted towards lower wavelengths compared with pure hematite. According to the XRD data, these positions between 534 and 537 nm correspond to Al-substitution in hematite of about 6.7 mole%. KOSMAS et al. (1986; Fig. 2) reported second derivative minima at approximately 557 and 539 nm for synthetic hematites with Al-amounts of 6.3 and 12.5 mole%. Despite the fact that Al-substitution in natural and synthetic hematites causes a shift towards lower wavelength, a correlation between Al-amount and minimum band position cannot be made. This suggests that parameters other than Al-substitution (e.g. particle size, strain) can affect the band position for hematite. In addition, the method of band position measurement may also introduce errors. As consequence, further calibration is necessary to accurately analyze the positions of second-derivative bands in order to correlate them with Al-substitution.

Magnetic analysis reveals the presence of magnetite and/or maghemite as a third ferric mineral phase in all samples, except the one from the pallid zone. Since both mineral phases have a very similar low coercivity behavior, an unambiguous assignment cannot be made by IRM. The comparison of magnetic and spectroscopic data, however, excludes the presence of maghemite, since no characteristic splitting of the $2(^6A_1) \rightarrow 2(^4T_1(^4G))$ transition that generally results in absorption bands at 495 and 512 nm (MALENGREAU et al., 1994) was found. Hence, the low coercivity phase in the laterite profile can unambiguously be attributed to magnetite. This agrees well with magnetic data of GEHRING et al. (1992), which show that magnetite is lithogenic and unevenly distributed in the duricrust.

Conclusions

The combined application of mineralogical and magnetic methods with diffuse reflectance spectroscopy to samples from a laterite profile leads to the following conclusions:
- Diffuse reflectance spectroscopy and IRM can identify all naturally occurring ferric oxides, but the determination of Al for Fe substitution in these oxides is limited.
- There is a correlation of Al-substitution with the shift of diagnostic bands in the diffuse reflectance spectra of natural goethites.
- An unambiguous correlation of Al for Fe substitution in hematite and the shift of the diagnostic band in the diffuse reflectance spectra cannot be made before more calibration data are available.

References

BARRON, V., RENDON, J.L., TORRENT, J. and SERNA, J. (1984): Relation of infrared, crystallochemical, and morphological properties of Al-substituted hematites. Clays Clay Miner., 32, 475–479.
BERRY, L., POST, B., WEISSMANN, S. and MCMURDIE, H. (1986): JCPDS – Mineral Powder Diffraction File. International Center for Diffraction Data. Swarthmore Pennsylvania, U.S.A., 1396 pp.
BISH, D. and JONES, R. (1991): Quantitative X-ray diffraction analysis of soils; comparison of convential curve-fitting and Rietveld full-pattern methods. In

Program and Abstract, Clay Miner. Soc., 28th meeting, p. 16.

CAHILL, J.E. (1979): Derivative spectroscopy: Understanding its application. Amer. Lab., 79–85.

COEY, J.M.D. (1988): Magnetic properties of iron in soil iron oxides and clay minerals. In: STUCKI, J.W., GOODMAN, B.A. and SCHWERTMANN, U. (eds): Iron in soils and clay minerals. Reidel, Dordrecht, 397–466.

DUNFIELD, L.G. and READ, J.F. (1972): Determination of reaction rates by the use of cubic spline interpolation. J. Chem. Phys., 57, 2178–2183.

GEHRING, A.U. and KARTHEIN, R. (1990): An ESR and calorimetric study of iron oolitic samples from the Northampton ironstone. Clay Min., 25, 303–411.

GEHRING, A.U., KELLER, P. and HELLER, F. (1992): Magnetic evidence for the origin of lateritic duricrusts in southern Mali (West Africa). Palaeogeogr., Palaeoclimat., Palaeoecol., 95, 33–40.

GEHRING, A.U., FRY, I.V., LUSTER, J. and SPOSITO, G. (1993): Vanadium (IV) in a multimineral lateritic saprolite: A thermoanalytical and spectroscopic study. Soil Sci. Soc. Amer. J., 57, 868–873.

GEHRING, A.U., LANGER M.R. and GEHRING C.A. (1994): Ferriferous bacterial incrustations in lateritic duricrusts from Southern Mali (West Africa). Geoderma, 61, 213–222.

HUGHES, J.C. (1982): High gradient magnetic separation of some soil clays from Nigeria, Brazil and Colombia. I. The interrelationships of iron and aluminium extracted by acid ammonium oxalate and carbon. J. Soil Sci., 33, 509–519.

HUGUENIN, R.L. and JONES, J.L. (1986): Intelligent information extraction from reflectance spectra: absorption band positions. J. Geophys. Res., 91, 9585–9598.

HUNT, G.R., SALISBURY, J.W. and LENHOFF, C.J. (1971): Visible and near-infrared spectra of minerals and rocks. III. Oxides and hydroxides. Mod. Geol., 2, 195–205.

KARICKHOFF, S.W. and BAILEY, G.W. (1973): Optical absorption spectra of clay minerals. Clays Clay Miner., 21, 59–70.

KOSMAS, C.S., FRANZMEIER, D.P. and SCHULZE, D.G. (1986): Relationship among derivative spectroscopy, color, crystallite dimensions and Al-substitution of synthetic goethites and hematites. Clays Clay Miner., 34, 625–634.

MALENGREAU, N., MULLER, J.-P. and CALAS, G. (1994): Fe-speciation in kaolins: a diffuse reflectance study. Clays Clay Miner., 42, 137–147.

MALENGREAU, N., MULLER, J.-P. and CALAS, G. (1995): Spectroscopic approach of Ti status and mobility in kaolinitic samples. Clays Clay Miner., 43, 615–621.

NAIDU, S.V.N. and HOUSKA, C.R. (1982): Profile separation in complex powder patterns. J. Appl. Cryst. 15, 190–198.

NORRISH, K. and TAYLOR, R.M. (1961): The isomorphous replacement of iron by aluminum in soil goethite. J. Soil Sci., 12, 294–306.

REINSCH, C.H. (1967): Smoothing by spline functions. Numer. Math., 10, 177–183.

SCHNEIDER, J. (1987): Rietveld methods runs on IBM-AT. Acta Cryst. A43, suppl. C, 295.

SCHWERTMANN, U. (1964): Differenzierung der Eisenoxide des Bodens durch photochemische Extraktion mit saurer Ammoniumoxalat-Lösung. Z. Pflanzenernähr. Bodenk., 105, 194–202.

SCHWERTMANN, U. (1988): Occurrence and formation of iron oxides in various pedoenvironments. In: STUCKI, J.W., GOODMAN, B.A. and SCHWERTMANN, U. (eds): Iron in soils and clay minerals. Reidel, Dordrecht, 267–308.

SCHWERTMANN, U. and CARLSON, L. (1994): Aluminum influence on iron oxides: XVII. Unit cell parameters and aluminum substitution of natural goethites. Soil Sci. Soc. Am. J., 58, 256–261.

SHERMAN, D.M. and WAITE, D. (1985): Electronic spectra of Fe^{3+} oxides and oxide hydroxides in the near IR to the near UV. Am. Miner., 70, 1262–1269.

SNETSINGER, K.G. (1966): Barium-vanadium muscovite and vanadium tourmaline from Mariposa County, California. Am. Miner., 51, 1623–1639.

STANJEK, H. and SCHWERTMANN, U. (1992): The influence of aluminum on iron oxides. Part XVI: hydroxyl and aluminum substitution in sythethic hematites. Clays Clay Miner., 40, 347–354.

TARDY, Y. and NAHON, D. (1985): Geochemistry of laterites, stability of Al-goethite, Al-hematite, and Fe^{3+}-kaolinite in bauxites and ferricretes: An approach to the mechanism of concretion formation. Am. J. Sci., 285, 865–903.

YOUNG, R. (1993): The Rietveld Method. International Union of Crystallography, Oxford University Press, Oxford; 297 pp.